Generation of higher-order atomic dipole squeezing in a high-Q micromaser cavity: VIII. multi-photon interaction

Rui-Hua Xie^{a*} and Qin Rao^b

^aDepartment of Chemistry, Queen's University, Kingston, ON K7L 3N6, Canada;

^bDepartment of Engineering Physics, Queen's University, Kingston, ON K7L 3N6, Canada

(November 5, 2018)

Abstract

In our preceding serial works, we have investigated the generation of higherorder atomic dipole squeezing (HOADS) in a high-Q micromaser cavity, discussing the effects of dynamic Stark shift, atomic damping, atomic coherence and nonlinear one-photon processes and different initial states (for example, correlated and uncorrelated states, superposition states, squeezed vacuum). In this paper, we continue to study HOADS in a high-Q micromaser cavity, but consider that the atom interacts with the optical field via a multi-photon transition process and that the initial atom is arbitrarily prepared. For a vacuum initial field, we demonstrate that HOADS cannot occur if the atom is initially prepared in a chaotic state and that a coherent atomic state generates less efficient and stable HOADS than an arbitrary one. It is found that large detuning may lead to enhanced and strong HOADS.

PACS (numbers): 42.50.Dv, 42.50.Lc, 32.80.-t

Keywords: Dipole; Squeezed state; Chaotic state; Vacuum field; Multiphoton transition; Quantum fluctuation; Uncertainty relation; Density matrix method.

^{*}Email: rhxie@titan.nist.gov; Phone: (301) 975-5159; Fax: (301) 990-1350

1. INTRODUCTION

In 1926, Heisenberg [1] proposed a fundamental, general principle of nature, known as Heisenberg uncertainty principle. Although this principle is of no consequence for the macroscopic world, it does play an important role in dealing with problems met in the microscopic world (for example, atom, molecule, nanocrystals, solid, and so on). It was Kennard [2] who presented us the first example of nonclassical states, called squeezed state, in which the quantum fluctuations in a dynamical observable may be reduced below the standard quantum limit at the expense of increased fluctuations in its canonical conjugated one without violating the Heisenberg uncertain principle. Furthermore, Plebański [3] made an important contribution to the theory of squeezed states in 1956. The exciting and constructive experimental results of the first successful generation and detection of squeezed states was reported in the middle of the 1980's [4]. Since then, the squeezed states have been extensively studied, both theoretically and experimentally [5–17], due to their potential applications in quantum communication, high-resolution laser spectroscopy measurement, gravity wave detection and quantum information theory (quantum teleporation, dense coding, cryptography, quantum nondemolition measurement and power-recycled interferometer). These extensive studies have shown that a lot of nonlinear optical systems could generate squeezed states for the field and atom, for example, in two-photon laser, parametric amplifiers, four-wave mixing, resonance fluorescence, Rydberg atom maser and cooperative Dicke system. A general relationship between field and atomic dipole squeezing has even been established under different initial conditions for both the field and atom [5,8,10-12].

Recently, the rapid development of techniques for making higher-order correlation measurements has resulted in an increased interest in generating another kind of nonclassical states, known as higher-order squeezed states [18]. In these states, higher-order quantum fluctuations in one quadrature of the field or atomic dipole could be reduced without violating higher-order uncertainty relations [18]. It has been predicted that higher-order squeezed states for the radiation In 1997, one of us, Xie, with his colleagues [19] introduced the concept of higher-order atomic dipole squeezing (HOADS) and applied it to high-Q micromaser cavities. In our serial works |20-25|, we have discussed thoroughly the important connection of HOADS with the second-order field and atomic dipole squeezing (ADS), the effects of a nonlinear one-photon process and dynamical Stark shift in two-photon processes on HOADS, and different initial conditions regarding both the atomic and field (for example, uncorrelated and correlated coherent states, superposition states, squeezed vacuum). These extensive studies have made an important contribution to the theory of higher-order squeezed states and provided us an approach to extracting information efficiently from an optical signal by higher-order correlation measurements. However, the initial conditions are more or less individualized, and only one- and two-photon transitions have been investigated. Hence, it is our purpose in this paper to treat this problem in a more general way. As a first step, we consider that the initial atom is arbitrarily prepared and that the atom interacts with the field via a multi-photon transition process. In this paper, we use the twolevel multi-photon Jaynes-Cummings model [9,26,27] and utilize the density matrix method which can describe very well arbitrary atomic-field states such as a mixed state. Their actual squeezing conditions and behaviours were carefully discussed.

This paper is organized as follows. In section 2, we describe the theoretical model of multi-photon interaction between a cavity field and a two-level atom and introduce the concept of HOADS. In section 3, assuming that the atom is initially prepared in an arbitrarily state, we investigate the generation of HOADS in the multi-photon Jaynes-Cummings model. A summary is given in the last section.

2. THEORY

Here we consider the interaction of a two-level atom with a single-mode quantized field involving the emission or absorption of multi-photons per atomic transition. The Hamiltonian of this system can be written as follows

$$H = \Omega a^{\dagger} a + \omega S_z + \epsilon (a^{\dagger\xi} + a^{\xi})(S_- + S_+)$$
(1)

which is the multi-photon Jaynes-Cummings model without the rotating-wave approximation (RWA) [9,26]. If the RWA is explicitly used, then we have

$$H = \Omega a^{\dagger}a + \omega S_z + \epsilon (a^{\dagger\xi}S_- + a^{\xi}S_+)$$
⁽²⁾

which is the multi-photon Jaynes-Cummings model within the RWA [27]. S_z and S_{\pm} are operators of the atomic pseudospin inversion and transition, respectively, and satisfy the commutation [7]: $[S_+, S_-] = 2S_z$ and $[S_z, S_{\pm}] = \pm S_{\pm}$. ω is the transition frequency for the atom. a^{\dagger} and a are the creation and annihilation operators for the photons with the frequency Ω , which obey the boson operators' commutation relations, $[a, a^{\dagger}] = 1$. ϵ is the coupling constant between the atom and the radiation field, and ξ is the absorbing or emitting photon numbers per atomic transition. Throughout we employ the unit with $\hbar = c = 1$.

In order to investigate the squeezing properties of the atomic dipole variables, we follow the standard procedure of defining the slowly varying operators [7]

$$S_x = \frac{1}{2} \left[S_+ e^{-i\omega t} + S_- e^{i\omega t} \right],$$
(3)

$$S_y = \frac{1}{2i} \left[S_+ e^{-i\omega t} - S_- e^{i\omega t} \right],\tag{4}$$

where S_x and S_y , in fact, correspond to the dispersive and absorptive components of the slowly varying atomic dipole [28], respectively. One can easily show that the above operators obey the commutation relation, $[S_x, S_y] = iS_z$. Correspondingly, we found the higher-order uncertainty relation [19] concretely given by

$$(\Delta S_x)^P (\Delta S_y)^P \ge \frac{1}{4} \left| [(\Delta S_x)^{P/2}, (\Delta S_y)^{P/2}] \right|^2.$$
 (5)

For a two-level atom, we have

$$(\Delta S_j)^P = 2^{-P} + \sum_{k=2,4,\dots}^P (C_P^k - C_P^{k-1}) 2^{k-P} < S_j >^k \qquad (j = x, y), \tag{6}$$

$$[(\Delta S_x)^{P/2}, (\Delta S_y)^{P/2}] = i < S_z > \sum_{m,n}^{P/2-1} C_{P/2}^m C_{P/2}^n 2^{2-P+m+n} < S_x >^m < S_y >^n,$$
(7)

where $P/2 \ge 1$ is an integer. If P/2 is even (odd), then m and n are odd (even) numbers. It is convenient that we define the following functions

$$F_1(P) = (\Delta S_x)^P - \frac{1}{2} \left| [(\Delta S_x)^{P/2}, (\Delta S_y)^{P/2}] \right|,$$
(8)

$$F_2(P) = (\Delta S_y)^P - \frac{1}{2} \left| [(\Delta S_x)^{P/2}, (\Delta S_y)^{P/2}] \right|.$$
(9)

Then, higher-order quantum fluctuations in the component S_x (or S_y) of the dipole are squeezed if $F_1 < 0$ (or $F_2 < 0$). This is the general definition of HOADS [19].

3. Results

We denote $|n\rangle$ as the Fock state of the radiation field and $|+\rangle$ and $|-\rangle$ as the excited and ground states of the two-level atom, respectively. Using the standard bare-state procedure introduced by Xie *et al.* [29], we can calculate the density operator of the atom-field coupling system at time *t* with an arbitrary initial condition $\rho(t = 0)$ by

$$\rho(t) = U(t)^{\dagger} \rho(t=0) U(t) \equiv \sum_{ij} \rho_{ji}(0) e^{-i(E_i - E_j)t} | j \rangle \langle i |$$
(10)

where $\rho_{ji}(0) = \langle j \mid \rho(0) \mid i \rangle$. $\mid i \rangle$ and E_i are the *i*th eigenstate and its corresponding eigenvalue, respectively, and $U(t) = \exp(-iHt)$ is the unitary evolution operator. Therefore, the expectation value of any physical operator O at time t can be arrived at through

$$\langle O(t) \rangle = Tr[\rho(t)O(0)] = \sum_{i} \langle i \mid \rho(t)O(0) \mid i \rangle$$
$$= \sum_{ij} \rho_{ij}(t) \langle j \mid O(0) \mid i \rangle = \sum_{n=0}^{\infty} \sum_{m=0}^{\infty} \sum_{\alpha=1}^{2} \sum_{\beta}^{2} \rho_{n\alpha,m\beta}(t) \langle \Psi_{m,\beta} \mid O(0) \mid \Psi_{n,\alpha} \rangle,$$
(11)

where $|i\rangle = \sum_{n=0}^{\infty} \sum_{\alpha=1}^{2} |\Psi_{n,\alpha}\rangle$. Here $|\Psi_{n,\alpha}\rangle$ denotes the dressed state with *n* being the photon number of the optical field. The wave function $|\Psi_{n,\alpha=1,2}\rangle$ can be expressed by

$$|\Psi_{n,1}\rangle = (|+,n\rangle + |-,n+p\rangle)/\sqrt{2},$$
(12)

$$|\Psi_{n,2}\rangle = (|+,n\rangle - |-,n+p\rangle)/\sqrt{2}$$
(13)

with the corresponding eigenenergies

$$E_{n,1} = (n + \xi/2)\omega + \epsilon \Pi_n, \tag{14}$$

$$E_{n,2} = (n + \xi/2)\omega - \epsilon \Pi_n, \tag{15}$$

where Π_n is defined by

$$\Pi_n = \sqrt{\frac{(n+\xi)!}{n!}}.$$
(16)

As usual, we assume that the initial density matrix $\rho(t = 0)$ can be decomposed into its atomic and field parts, i.e., $\rho(0) = \rho_a(0) \otimes \rho_f(0)$. In this paper, we assume that the initial atomic state is arbitrarily prepared, i.e.,

$$\rho_a(0) = \sin^2 \theta \mid + \rangle \langle + \mid + \cos^2 \theta \mid - \rangle \langle - \mid + \eta \left(e^{-i\phi} \mid - \rangle \langle + \mid + e^{i\phi} \mid + \rangle \langle - \mid \right)$$
(17)

with

$$\eta^2 \le \sin^2 \theta \cos^2 \theta \le \frac{1}{4},\tag{18}$$

and the field is in its vacuum state, i.e.,

$$\rho_f(0) = \mid 0 \rangle \langle 0 \mid . \tag{19}$$

Then, we have arrived at the expectation values of S_x , S_y and S_z

$$\langle S_x(t) \rangle = \eta \left\{ \cos(\Gamma\tau) \cos\left(\frac{\Delta}{2}\tau + \phi\right) - \Delta \frac{\sin(\Gamma\tau)}{2\Gamma} \sin\left(\frac{\Delta}{2}\tau + \phi\right) \right\},\tag{20}$$

$$< S_y(t) > = \eta \left\{ \cos(\Gamma\tau) \sin\left(\frac{\Delta}{2}\tau + \phi\right) - \Delta \frac{\sin(\Gamma\tau)}{2\Gamma} \cos\left(\frac{\Delta}{2}\tau + \phi\right) \right\},\tag{21}$$

$$\langle S_z(t) \rangle = \frac{1}{2} \left\{ \sin^2 \theta \frac{\Delta^2 / 4 + \xi! \cos(2\Gamma\tau)}{\Gamma^2} - \cos^2 \theta \right\},\tag{22}$$

where $\tau = \epsilon t$ is the scaled interaction time, $\Delta = (\xi \Omega - \omega)/\epsilon$ is the scaled detuning, $\Gamma = \sqrt{\Delta^2/4 + \xi!}$ is the scaled Rabi frequency and ϕ is the relative phase between the excited state $|+\rangle$ and the ground state $|-\rangle$ of the two-level atom. If we take $\eta = \sin \theta \cos \theta$, the above results are in agreement with those of Xie *et al.* [9,26].

If the two-level atom is initially prepared in a chaotic state (i.e., $\eta = 0$), one can easily see that the second- and higher-order quantum fluctuations in S_x or S_y cannot be squeezed. In the case of pure initial atomic states, which still keep all the relevant physical features, we have $\eta = |\sin(2\theta)|/2$ and find that no HOADS occurs for a completely excited or ground atom, but HOADS could appear for a coherent atom as shown below.

One interesting result is the so-called population trapping [30], in which the expectation value of S_z takes on a steady value, i.e., $d < S_z(t) > /dt = 0$. This results in $\sqrt{\xi!}\tau = k\pi$ or $(k + 1/2)\pi$ (k=0, 1, 2, ...). Obviously, for $\sqrt{\xi!}\tau = (k + 1/2)\pi$, the second- and higher-order quantum fluctuations in S_x or S_y cannot be squeezed. However, for $\sqrt{\xi!}\tau = k\pi$, HOADS occurs for proper choice of the parameters η , θ and ϕ . Details are given below.

In Fig.1, we show a 3D contour plot for the function $F_1(P = 6)$, θ and η for $\phi = (k+1/2)\pi$ (k=0,1,2,...) in the case of resonance. We find that for $0 < \eta \le 0.5$ the sixth-order quantum fluctuations in S_x can be squeezed by properly choosing the parameter θ . Especially, when $\eta = 0.5$, HOADS appears almost in the whole range of θ except a small range around $\theta = \pi/4$ or $\theta = 3\pi/4$. Also it is obvious that the pure atomic state with $\eta = |\sin(2\theta)|/2$ generates less HOADS than the atomic state with $0 < \eta \le 0.5$. However, as we vary the phase to $\phi = k\pi$ (k=0,1,2,...), as shown in Fig.2, there exists only a small region of HOADS in the η - θ parameter space. This implies that HOADS is much sensitive to the relative phase between the excited and ground states of the two-level atom.

In Fig.3 and 4, we show 3D contour plots for the function $F_1(P = 6)$, parameter θ and phase ϕ for $\eta = |\sin(2\theta)| / 2$ and $\eta = 0.5$, respectively, for a resonance transition (i.e., $\Delta = 0$). HOADS patterns are clearly shown in the θ - ϕ parameter space. We find that HOADS is much sensitive to the phase for an initial pure atomic state, whereas it is relatively stable with respect to the phase for an arbitrary state with $\eta = 0.5$. This implies that an arbitrary atomic state could generate much efficient and stable HOADS than a pure one.

In Fig.5, we show the time evolution of the function $F_1(P = 6)$ for $\theta = \pi/2$, $\eta = 0.5$, $\phi = k\pi$ in the case of resonance. We notice that increasing the photon number ξ results in a decrease of the HOADS duration, which is inversely proportional to $\sqrt{\xi!}$. The HOADS frequency is directly proportional to $\sqrt{\xi!}$. In Fig.6, we show the time evolution of the function $F_1(P = 6)$ for $\theta = \pi/2$, $\eta = 0.5$ and $\phi = k\pi$ and $\Delta = 0, 1, 5$ in the case of one-photon transition. It is seen that the duration, period and strength of HOADS are much sensitive to the detuning. Especially, for a large detuning, for example $\Delta = 5$, we observe enhanced and strong HOADS. Similar results, as shown in Fig.7, are obtained for three-photon transition processes. These results show that large detuning can generate efficient HOADS than the resonance case.

Finally, it would be interesting to examine the relation between the second-order ADS (SOADS) and HOADS. In Fig.8 and 9, we show 3D contour plots for the function $F_2(P = 2)$, θ and ϕ for $\eta = |\sin(2\theta)|/2$ and $\eta = 0.5$, respectively, for a resonance transition. Comparing Fig.8 and 9 with Fig.3 and 4, respectively, we find that there exist additional θ - ϕ parameter regions where HOADS could occur but SOADS could not. There are also more HOADS dips than SOADS. For an arbitrary atomic state with $\eta = 0.5$, we see that HOADS with respect to the fluctuation of the phase ϕ is much stable than SOADS. Certainly, as demonstrated in our previous serial works [20–25], there exist common θ - ϕ parameter regions where both HOADS could be generated in the mean time.

4. SUMMARY

In summary, we study HOADS in a high-Q micromaser cavity by considering a twoleve atom interacting with an optical field through a multi-photon transition. Assuming that the initial atom is arbitrarily prepared and the field is initially in a vacuum state, we demonstrate that HOADS cannot appear if the atom is initially prepared in a chaotic state and that a coherent atomic state could generate less efficient and stable HOADS than an arbitrary one. It is found that large detuning may lead to enhanced and strong HOADS.

ACKNOWLEDGEMENT

We would like to thank Jianing Colin for some important contribution and constructive conversation and encouragement. One of us (Q. R.) acknowledges the Reinhart Fellowship provided by Queen's University for financial support.

REFERENCES

- [1] W. Heisenberg, Z. Phys. B 43 (1927) 172.
- [2] E. H. Kennard, Z. Phys. B 44 (1927) 326.
- [3] J. Plebański, Phys. Rev. 101 (1956) 1825.
- [4] R. E. Slusher, W. Hollberg, B. Yurke, J. C. Mertz, J. F. Valley, Phys. Rev. Lett. 55 (1985) 2409.
- [5] K. Wodkiewicz, P. L. Knight, S. J. Buckle, S. M. Barnett, Phys. Rev. A 35 (1987) 2567.
- [6] C. Fabre, E. Giacobino (eds), Appl. Phys B: Photophys. Laser Chem. 55 (1992) 189, one special issue on quantum noise reduction in optical systems/experiments.
- [7] R. H. Xie, G. O. Xu, D. H. Liu, Phys. Lett. A 202 (1995) 28.
- [8] R. H. Xie, Phys. Rev. A 53 (1996) 2897.
- [9] R. H. Xie, D. H. Liu, G. O. Xu, Z. Phys. B 99 (1996) 253
- [10] R. H. Xie, X. H. Wu, D. H. Liu, G. O. Xu, Z. Phys. B 101 (1996) 247.
- [11] R. H. Xie, G. O. Xu, Phys. Rev. E 54 (1996) 1402.
- [12] Y. T. Zou, R. H. Xie, C. D. Gong, Z. Phys. B 101 (1996) 425.
- [13] G. Breitenbach, S. Schiller, J. Mlynek, Nature (London) 387 (1997) 471.
- [14] A. Furusawa, J. Sorensen, S. L. Braunstein, C. A. Fuchs, H. J. Kimble, E. S. Polzik, Science 282 (1998) 706.
- [15] H. A. Haus, Electromagnetic Noise and Quantum Optical Measurements (Springer-Verlag, Berlin, 2000).
- [16] R. H. Xie, Phys. Rev. A 62 (2000) 017801.
- [17] R. H. Xie, Phys. Rev. A 65 (2002) 055801.

- [18] C. K. Hong, L. Mandel, Phys. Rev. A 32 (1985) 974.
- [19] R. H. Xie, R. B. Tao, G. O. Xu, Physica A 246 (1997) 529.
- [20] R. H. Xie, V. H. Smith, Jr., Physica A, 301 (2001) 114.
- [21] R. H. Xie, V. H. Smith, Jr., Physica A, 301 (2001) 129.
- [22] R. H. Xie, V. H. Smith, Jr., Physica A 307 (2002) 207.
- [23] R. H. Xie, Q. Rao, Physica A, PHYSA 6778.
- [24] R. H. Xie, Q. Rao, Physica A, PHYSA 6779.
- [25] R. H. Xie, Q. Rao, Physica A, PHYSA 6780.
- [26] R. H. Xie, Q. Rao, D. H. Liu, G. O. Xu, IL Nuovo Cimmento D 18 (1996) 405
- [27] C. V. Sukumar, D. Buck, Phys. Lett. A 83 (1981) 211.
- [28] N. B. Narozhny, J. J. Sanchez-Mondragon, J. H. Eberly, Phys. Rev. A. 23 (1981) 236.
- [29] R. H. Xie, G. O. Xu, D. H. Liu, Commun. Theor. Phys. 27 (1997) 265.
- [30] J. I. Cirac, L. L. Sanchez-Soto, Phys. Rev. A 42 (1990) 2851.

Caption of Figures

FIG.1: The 3D contour plot of function $F_1(P = 6)$, η and θ for $\Delta = 0$, $\sqrt{\xi!}\tau = k\pi$ and $\phi = (k + 1/2)\pi$ (k=0,1,2,...), where the dotted line is for $F_1(P = 6) = 0$, the dotted-dashed lines for $F_1(P = 6) = 0.01$, and the dashed lines for $F_1(P = 6) < 0$ in the range of -0.045 to -0.005 with an interval of 0.005. The solid line is for $\eta = |\sin \theta \cos \theta|$.

FIG.2: The 3D contour plot of function $F_1(P = 6)$, η and θ for $\Delta = 0$, $\sqrt{\xi!}\tau = k\pi$ and $\phi = k\pi$ (k=0,1,2,...), where the dotted line is for $F_1(P = 6) = 0$, the dotted-dashed lines for $F_1(P = 6) > 0$ in the range of 0.01 to 0.05 with an interval of 0.01, and the dashed lines for $F_1(P = 6) < 0$ in the range of -0.06 to -0.005 with an interval of 0.005. The solid line is for $\eta = |\sin \theta \cos \theta|$.

FIG.3: The 3D contour plot of function $F_1(P = 6)$, ϕ and θ for $\Delta = 0$, $\sqrt{\xi!}\tau = k\pi$ and $\eta = |\sin\theta\cos\theta|$, where the dotted line is for $F_1(P = 6) = 0$, the dotted-dashed lines for $F_1(P = 6) > 0$ in the range of 0.01 to 0.05 with an interval of 0.01, and the solid lines for $F_1(P = 6) < 0$ in the range of -0.06 to -0.001 with an interval of 0.001.

FIG.4: The 3D contour plot of function $F_1(P = 6)$, ϕ and θ for $\Delta = 0$, $\sqrt{\xi!}\tau = k\pi$ and $\eta = 0.5$, where the dotted line is for $F_1(P = 6) = 0$, the dotted-dashed lines for $F_1(P = 6) > 0$ in the range of 0.01 to 0.05 with an interval of 0.01, and the solid lines for $F_1(P = 6) < 0$ in the range of -0.06 to -0.001 with an interval of 0.001.

FIG.5: Time evolution of the function $F_1(P = 6)$ for $\eta = 0.5$, $\theta = \pi/2$, $\Delta = 0$ and $\phi = k\pi$ (k=0,1,2,...): (a) $\xi = 1$ (solid line); (b) $\xi = 4$ (dotted-dashed line).

FIG.6: Time evolution of the function $F_1(P = 6)$ for $\eta = 0.5$, $\theta = \pi/2$, $\phi = k\pi$

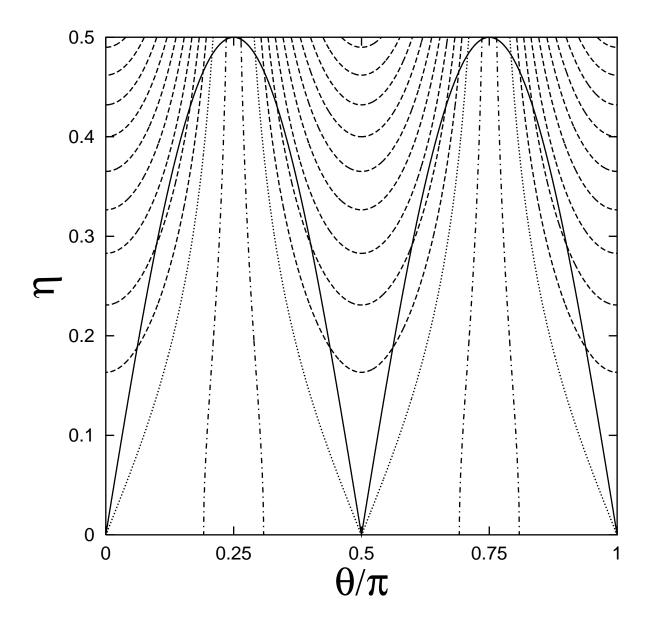
(k=0,1,2,...) and $\xi = 1$: (a) $\Delta = 0$ (dashed line); (b) $\Delta = 1$ (dotted-dashed line); (c) $\Delta = 5$ (solid line).

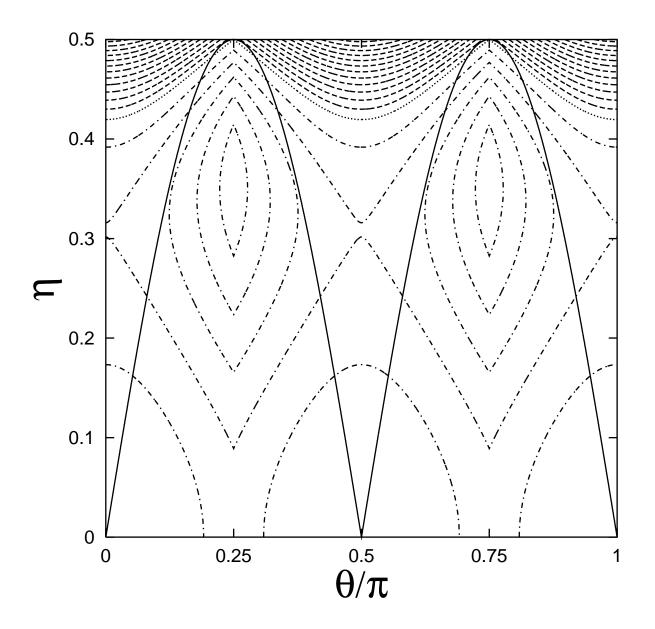
FIG.7: Time evolution of the function $F_1(P = 6)$ for $\eta = 0.5$, $\theta = \pi/2$, $\phi = k\pi$ (k=0,1,2,...) and $\xi = 3$: (a) $\Delta = 0$ (dashed line); (b) $\Delta = 1$ (dotted-dashed line); (c) $\Delta = 10$ (solid line).

FIG.8: The 3D contour plot of function $F_2(P = 2)$, ϕ and θ for $\Delta = 0$, $\sqrt{\xi!}\tau = k\pi$ and $\eta = |\sin\theta\cos\theta|$, where the dotted line is for $F_2(P = 2) = 0$, the dotted-dashed lines for $F_2(P = 2) > 0$ in the range of 0.01 to 0.24 with an interval of 0.01, and the solid lines for $F_2(P = 2) < 0$ in the range of -0.06 to -0.005 with an interval of 0.005.

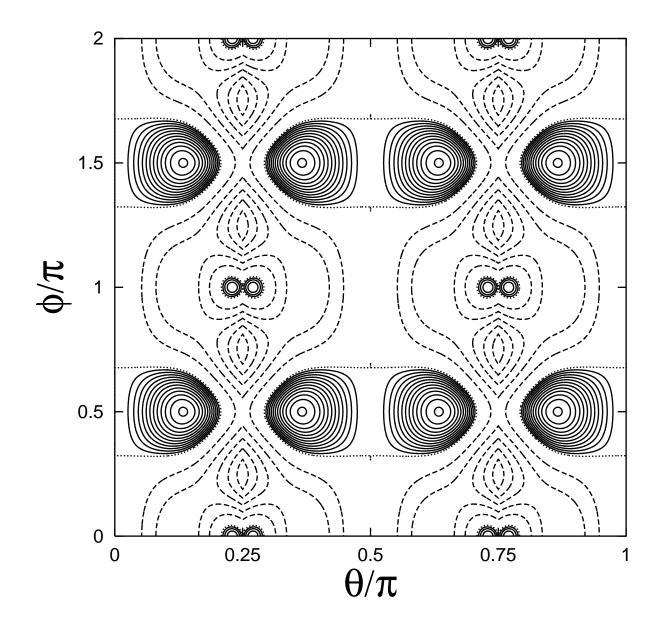
FIG.9: The 3D contour plot of function $F_2(P = 2)$, ϕ and θ for $\Delta = 0$, $\sqrt{\xi!}\tau = k\pi$ and $\eta = 0.5$, where the dotted line is for $F_2(P = 2) = 0$, the dotted-dashed lines for $F_2(P = 2) > 0$ in the range of 0.01 to 0.22 with an interval of 0.03, and the solid lines for $F_2(P = 2) < 0$ in the range of -0.24 to -0.01 with an interval of 0.01.

Xie & Rao: FIG.1/PHYSICA A

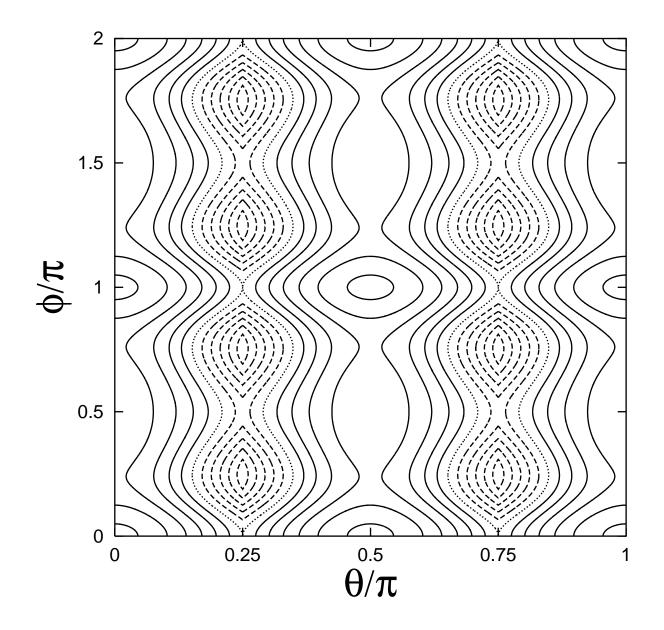


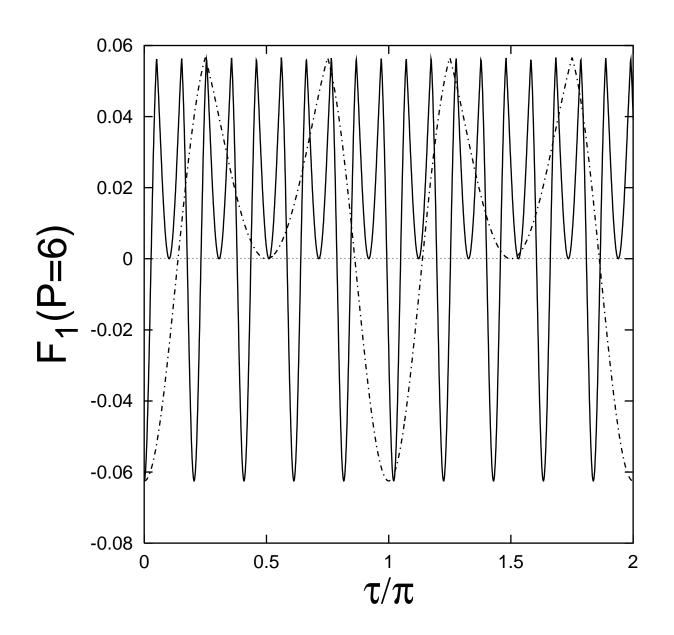


Xie & Rao: FIG.3/PHYSICA A

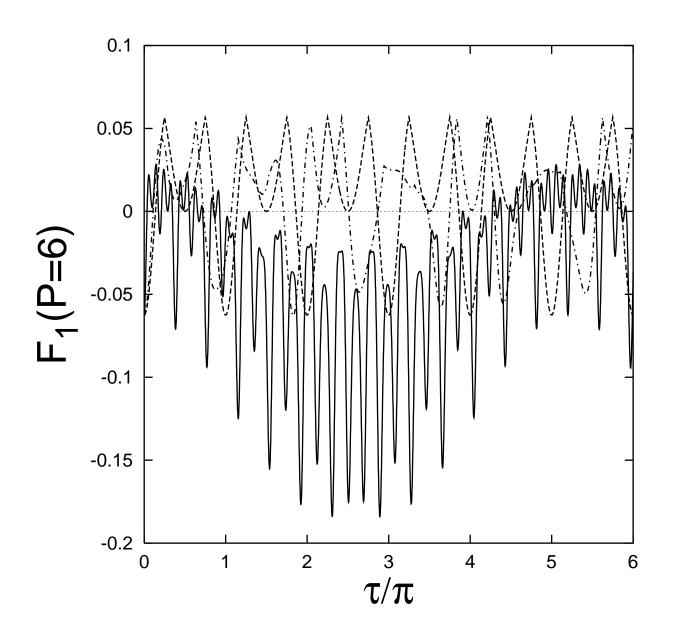


Xie & Rao: FIG.4/PHYSICA A





Xie & Rao: FIG.6/PHYSICA A



Xie & Rao: FIG.7/PHYSICA A

